Online resource 2

This file contains the description of the auxiliary experiment ran in a parallel microcosm experiment which aimed to detect potential macronutrient limitation of nitrate uptake.

Title: Disentangling effects of multiple agricultural stressors on benthic and hyporheic nitrate uptake

Journal name: Biogeochemistry

Authors: [1]Julia Pasqualini, [2]Daniel Graeber, [2]Alexander Bartusch, [3]Steffen Kümmel, [1]Zulma Lorena Duran Hernandez, [3,4]Niculina Musat, [2]Nergui Sunjidmaa, [1]Markus Weitere, [1]Mario Brauns

Email corresponding Author: julia.pasqualini@ufz.de

Author affiliation:

[1] Department of River Ecology, Helmholtz Centre for Environmental Research-UFZ, Brückstr. 3a, 39114, Magdeburg, Germany

[2]Department of Aquatic Ecosystem Analysis and Management, Helmholtz Centre for Environmental Research-UFZ, Brückstr. 3a, 39114, Magdeburg, Germany

[3]Department of Isotope Biogeochemistry, Helmholtz Centre for Environmental Research-UFZ, Permoserstraße 15, 04318 Leipzig, Germany

[4] Department of Biology, Section for Microbiology, Ny Munkegade 114, Aarhus University, Denmark

Auxiliary experiment in microcosms to detect potential macronutrient limitation of nitrate-N uptake

Background

Large-scale empirical studies linked DOC : nitrate-N ratios to nitrate-N concentrations and gross uptake, where low DOC : nitrate-N ratios coincided with low nitrate-N gross uptake

(Rodriguez-Cardona 2015; Rodríguez-Cardona et al. 2016) and high nitrate-N concentrations (Taylor and Townsend 2010; Helton et al. 2015). It furthermore, has been recently shown that the stoichiometric availability of DOC can stimulate stream benthic-biofilm (Stutter et al. 2020b) and hyporheic-sediment N and P assimilation (Stutter et al. 2020a), shifting nutrient losses from inorganic N and P to dissolved organic N (DON) and P (DOP) (Stutter et al. 2020a).

Clear predictions of microbial heterotrophic N assimilation may not always be derived when solely looking at DOC : nitrate-N ratios, as other dissolved N fractions, may also be important N sources for heterotrophs. It has been suggested that reactive macronutrients - those stimulating heterotrophic assimilation - include all forms of dissolved inorganic nitrogen (DIN, consisting of nitrate, nitrite, ammonium) and SRP, but also bioavailable forms of DOC, dissolved organic nitrogen (DON) and dissolved organic phosphorus (DOP) (Stutter et al. 2018). This macronutrient access hypothesis has been proven to give highly accurate estimates of carbon limitations of microbial, heterotrophic and aerobic nitrogen and phosphorus uptake in laboratory microcosm experiments (Graeber et al. 2021).

One major challenge in ecological stoichiometry is to simultaneously assess the effect of stoichiometric imbalances between the C : N : P of food sources, organisms, and the ecological functions exerted by the organisms. Ternary plots have been proposed to overcome this issue, where the authors normalized the C:N:P ratios of the target samples (e.g., water samples) to the Redfield ratio to assess stoichiometric limitations in eutrophication by using the Redfield ratio (106C : 16N : 1P) (Jarvie et al. 2018). However, using the Redfield ratio for heterotrophic microbial consumers is much less meaningful than using ratios specific to bacteria. To normalize the C:N:P ratio for bacteria, data from large-scale investigations of bacterial C : N : P could be used, such as Godwin and Cotner (Godwin and Cotner 2018), who found a median of 68C : 14N : 1P for 137 isolates of bacteria under

non-limited growth. A current study (Graeber et al. 2021) used such ternary plots and found high N and P uptake only in compartments with specific C:N:P (Fig. 1).

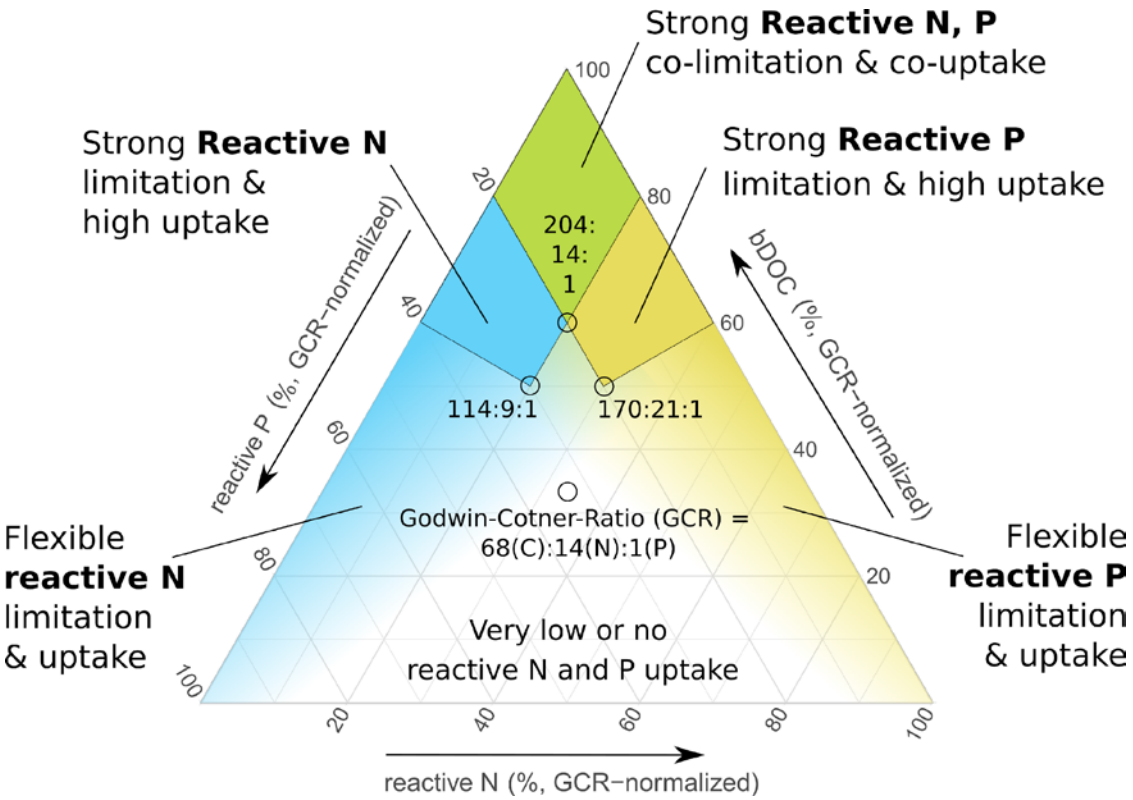

Fig. 1: Conceptual ternary plot with compartments constrained by the experimental results of Graeber et al. (2021). This plot describes specific bioavailable (b)DOC : reactive N (DIN plus bDON) and bDOC : reactive P ratios (determined as bDOC : SRP in this study) at which the authors find the highest reactive N uptake and reactive P uptake, a compartment with reactive N and P co-limitation, a compartment of flexible N and P uptake and a compartment without considerable reactive N and P uptake.

Hypothesis of sub-experiment

In addition to the effect of clogging reducing the available mass and the available oxygen for heterotrophic microbial assimilation, the system is impacted by N surplus, resulting in comparably high concentrations of nitrate-N. Furthermore, it is likely low in SRP concentration due to its forested catchment and steep slope. This may shift the bioavailable DOC : reactive N : reactive P towards N and P co-limitation, further limiting heterotrophic microbial N and P assimilation.

Methods

Experimental procedures

Water samples (500 mL) were taken from each flume at the flume outlet. The samples were stored cold for maximum 12 hours and filtered through pre-rinsed (200 mL DI and a small sample volume to prevent dilution) 47 mm diameter, 0.22 µm polycarbonate membrane (Membrapure, Gelman) filters to remove any bacteria. Here, a water sample was filtered for each of the 20 flumes at the start of the experiment (0 days) to compare to the concentration change at the end of the experiment (8 days, see also below).

For the bacterial inoculum, approximately 10 g of stream sediment (2 teaspoons from the source stream, not the flumes) were sampled in a 1 L bottle and filled up with 600 mL stream water (to prevent sediment drying). In the lab, this solution was gently shaken for 10 min or more and allowed to settle overnight. This bacterial inoculum was then filtered through a pre-rinsed (1 L DI water and a small sample volume to prevent dilution), Whatman GF/C filters (47 mm diameter, ~ 1.4 µm cutoff to keep bacteria but to remove most microbial primary producers) and then added to the samples before incubation (5 vol% of the sample) (Fellman et al. 2008).

The experiment was run in 20 250 mL glass vials (one per each of the 20 flumes with either control (C), fine sediment (FS), light and phosphorous (L&P) and fine sediment + light and phosphorous (L&P+FS) treatment), washed thoroughly with distilled water before the experiment. Here, an inoculum control with DI water and only bacterial inoculum is used to assess inoculum nutrient release (one sample at the start plus one sample at the end). Furthermore, a filtration and procedure control was run to check for impurities from the equipment. A sterile control was NOT conducted, as it is nearly impossible to get water samples sterile without affecting the DOM composition, and no non-biological effects on

DOM can be expected during dark incubations. Earlier studies on DOC bioavailability found no effects in sterile controls of stream DOC incubations over even 134 days (Qualls and Haines 1992).

The 250 mL white-glass vials were then put in the dark and constantly shaken at ~ 80 revolutions per minute at 16°C. After the experiment, DOC and nutrient concentrations were measured at the start of the experiment, after 8 days, a time at which previous, similar experiments have proven maximum bacterial reaction to Alder leaf leachate DOC and degradation of highly and medium labile DOC (Graeber et al. 2019), and less bioavailable DOC (Graeber et al. 2021). At the end of the experiment, all 21 samples (20 samples from the flumes + 1 sample to control for the bacterial inoculum effect on DOC and nutrient concentrations) taken from the experiment were filtered again with pre-rinsed 0.22 µm polycarbonate membrane filters (Membrapure, Gelman) before nutrient and DOC analysis.

The experiment ran for eight days. Flume samples were taken at the 25. May 2021, the experiment was started on the 26. May 2021. The experiment ended on the 03. June 2021.

For all filtration steps, a vacuum filtration system was used with not more than 200 mbar vacuum to prevent the destruction of microbial cells and lysis of organic matter into solution.

Measurements

We analysed the concentrations of ammonium-N, nitrite-N, nitrate-N and SRP by segmented-flow analysis (Skalar) photometrically, with quantification limits of 0.010, 0.006, 0.042 and 0.002 mgL^{-1}, respectively. We measured DOC as C_2 in the near IR after acidification stripping out the DIC by high-temperature catalytic oxidation (DIMATOC 2000 from DIMATEC, Germany), with a quantification limit of 0.50 mgL^{-1}. We determined total dissolved N (TDN) after persulfate oxidation photometrically as a nitrite-N complex in the

segment-flow analysis with a quantification limit of 0.084 mgL^{-1}. Here, we also determined total dissolved phosphorus (TDP) after oxidation of all P-containing compounds to SRP as organo-phosphorous complex photometrically (Hach DR 5000) with a quantification limit of 0.006 mgL^{-1}.

We used fluorescence-based excitation-emission matrices (EEMs, Horiba Aqualog, USA) measured in 1-cm Quartz glass cuvettes to assess the composition of DOM. We used an excitation range from 255 to 600 nm, and an emission range from 240 to 621 nm with an integration time of 0.72 s, medium CCD gain, an excitation increment of 5 nm, an emission increment of 0.82 nm, and an excitation slit width of 10 nm. With the same instrument, we measured the light absorbance from 255 to 600 nm to correct the inner-filter effect (Kothawala et al. 2013; Murphy et al. 2013). The absorbance was below 1 $c \quad ^{-1}$ at 240 nm, a range at which the inner-filter effect can be efficiently removed by the absorbance-based approach (Kothawala et al. 2013). Using the Raman scatter, fluorescence was normalized to Raman units (using the range of Raman scatter given in Lawaetz and Stedmon 2009)

Calculation of macronutrient limitation

The calculation of macronutrient limitation follows the approach of the macronutrient-access hypothesis, which is outlined in the introduction. Here, all bacterially available C, N and P fractions are included in the estimation of macronutrient limitation. In practice, we conducted the following data analysis steps (procedure as in Graeber et al. 2021):

1. Calculate DON and DOP, as $DON = totaldissolvednitrogen - (nitrate - N + nitrite - N + ammonium - N)$ and as $DOP = totaldissolvedphosphorus - solublereactivephosphorus$, respectively.

2. Calculate concentrations in cases where the measured variable concentrations were below the quantification limit. Here, I randomly sampled a number from a uniform distribution with an interval of 0 to the quantification limit for each occasion where a concentration was below the quantification limit. This approach is better than using half the quantification interval (it is more honest as it induces the true potential error of concentrations below the quantification limit for all subsequent calculations) and also needs to be used because a concentration smaller than the quantification interval is not equal 0 (Graeber et al. 2021).
3. Assess the error of DON and DOP via dissolved inorganic N (DIN) : total dissolved N (TDN) and SRP : total dissolved P (TDP) ratios and via the coefficient of variation (CV, calculated as $SD/mean$) of start DON and DOP concentrations (Graeber et al. 2012). Here, it is crucial for the final determination of potential macronutrient limitation to accurately estimate DON and DOP. Measurement errors can stack up towards high determination errors due to the indirect determination of DON and DOP. DIN:TDN ratios were below 0.8 and SRP:TDP ratios were below 0.9. Above DIN:TDN = 0.8 DON determination can be highly inaccurate due to problems with TDN measurements. Here, persulfate digestion was used before TDN measurements, which is usually coupled to relatively low TDN measurement errors (Lee and Westerhoff 2005). Since fewer variables need to be measured for DOP (only SRP and TDP) than for DON (all three DIN fractions plus TDN), the error for DOP is usually lower, despite the high SRP:TDP ratio. In the second step, I used the start DON and DOP concentrations to assess the determination errors of DON and DOP. These should be similar for each treatment, which was assessed using the treatment-wise CV. The maximum CV for DON was 0.13 (L&P treatment), and the maximum CV for DOP was 0.61 (L&P+FS treatment, the other treatments had a much lower CV).

Hence, I detected a high determination error for DOP, which was already indicated by the SRP:DOP ratio. However, the DOP concentrations were low (mean = 0.008 mgL^{-1}) in the mixed treatment (compared to SRP, mean = 0.04 mgL^{-1}), hence, I assumed that they would not impact the estimated final macronutrient limitation strongly.

4. Calculate the concentration of bioavailable DOC, DON and DOP per flume channel. Here, I calculated the concentration change between start (day 0) and end concentrations (day 8) for each flume channel, which is an experimental estimate of the amount of bioavailable DOC, DON and DOP.
5. The microbially (heterotrophic) reactive DOC equals the bioavailable DOC. In contrast, the microbially reactive N is the sum of the bioavailable DON and all DIN fractions, and the microbially reactive P is the sum of the bioavailable DOP and the SRP concentration. The reactive DOC, N and P were calculated for each flume channel.
6. To assess the relative C, N and P limitation, a ternary plot was used (see also the introduction). Here the C:N:P ratios of the reactive DOC, N and P were scaled to the C:N:P of the bacterial biomass, using the median estimate from a large-scale study by Godwin and Cotner (2018) (see also Graeber et al. 2021).

Extraction of DOM fluorophores

To assess whether any change in DOM composition was detected during the bioavailability experiment, a parallel factor analysis (PARAFAC) was employed to extract statistically independent DOM fluorophores. Here, we used the staRdom package in R (Pucher et al. 2019). To estimate the correct number of fluorophores, I used a combination of spectral shape assessment, split-half validation (four split-halves, 500 random restarts), and residual

fluorescence analysis (Murphy et al. 2013; Graeber et al. 2021). To get the final best model with the global minimum error, we ran the PARAFAC model with 500 restarts and chose the one with the minimum sum of squared errors (Murphy et al. 2013). Finally, we chose a model with three components, as the model became unstable with more components (Fig. 2).

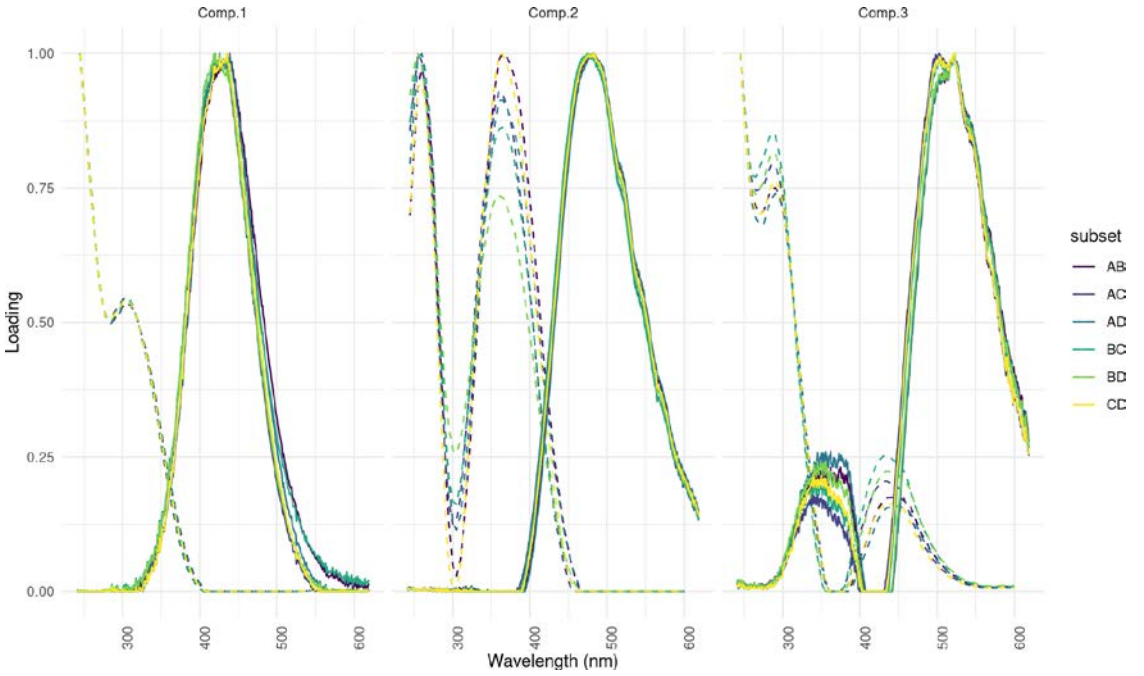

Fig. 2: Split-half validation plot. The solid lines are fluorophore emission spectra; the dashed lines are fluorophore excitation spectra. For this validation, the data is split into six parts with different mixtures of samples. If these parts produce similar models, the spectra overlap, and the PARAFAC model is assumed to be robust. Here, an additional statistic is calculated, Tucker's congruence coefficient (TCC). The TCC for all split-half spectra was > 0.98. Hence the spectra are highly similar.

Results and brief discussion

DOC reactivity

We found a high DOC concentration of on average 9.4 mg l^{-1}, which did not differ between treatments (Fig. 3 a). We also detected very low reactive DOC concentrations in terms of bioavailability for heterotrophic microbial degradation of, on average, 6.9%, apart from one outlier for the FS+L&P treatment (Fig. 3 b). However, since the reason for the sample is an outlier could not be assessed, the outlier sample was kept in all further analyses. Based on DOC concentration and DOC reactive, we calculate an average reactive DOC concentration of 0.6 mg L^{-1}.

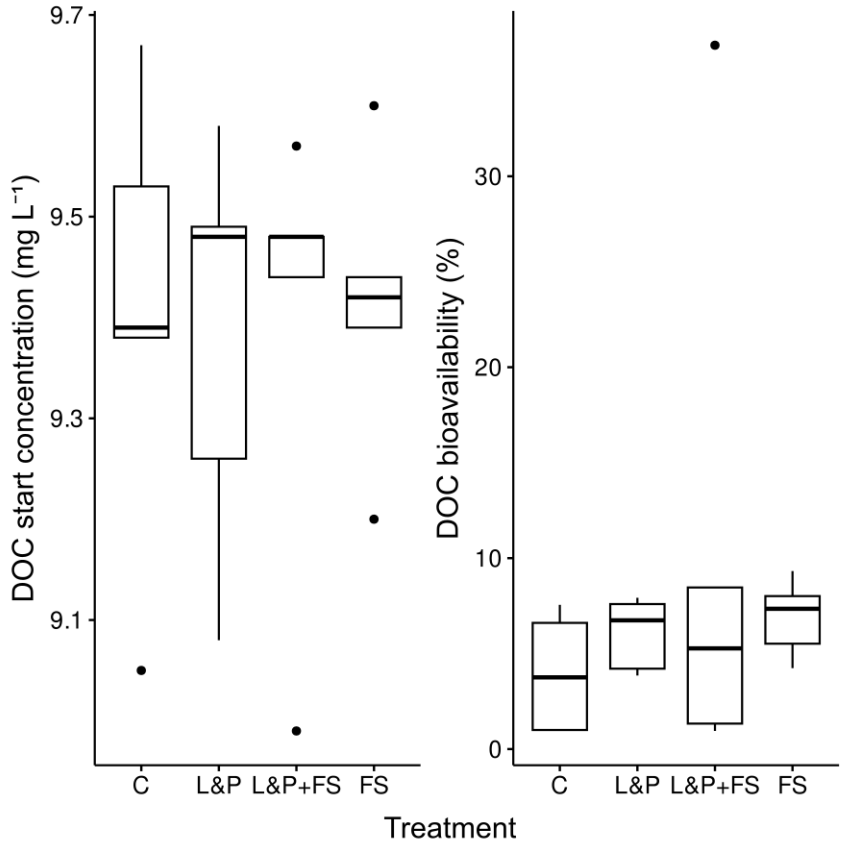

Fig. 3: DOC concentrations at the start (a.) and relative DOC bioavailability after eight days of incubation in the dark in microcosms (b.).

DOM composition change

The PARAFAC extracted three DOM fluorophores. C1 is a humic-acid-like fluorophore often assumed to be terrestrial plant-derived. C2 and C3 are two fulvic-acid-like fluorophores, especially the C3 is a ubiquitous fluorophore found in nearly all aquatic samples from soils to the marine realm.

We have not detected the removal of any fluorophore, instead, C1 was produced during the experiment (Fig. 4). This puts in doubt that this fluorophore is only a common humic-like terrestrial fluorophore and corroborates earlier findings that bacteria may indeed be able to produce humic-acid-like DOM out of aliphatic, labile DOC (Daoud and Tremblay 2019; Thompson and Cotner 2020).

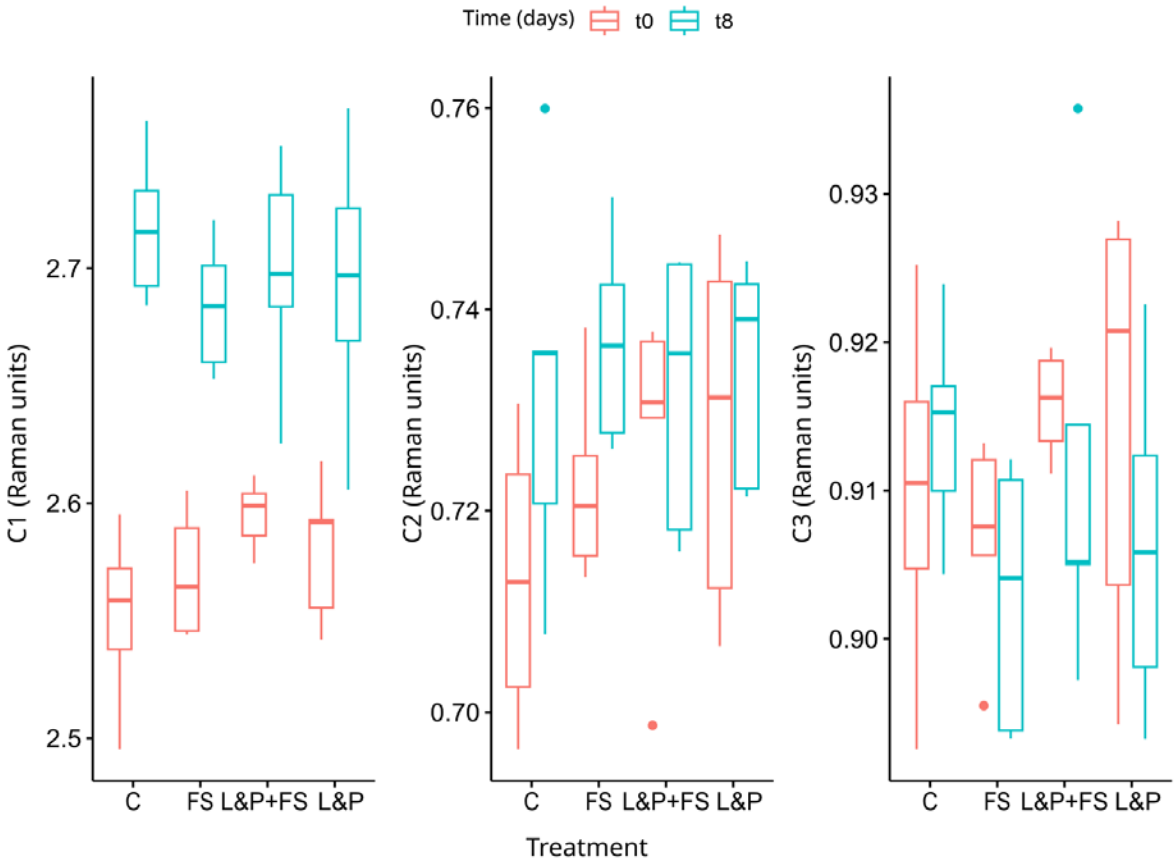

Fig. 4: DOM composition based on three DOM fluorophores extracted by PARAFAC. a. C1 is humic-acid-like often assumed to be plant-derived fluorophore b. & c. C2 and C3 are two fulvic-acid-like fluorophores, especially the C3 is a ubiquitous fluorophore found in nearly all aquatic samples from soils to the marine realm.

Macronutrient limitation of reactive N and P uptake

In Table 2 all the constituents to calculate reactive C : N : P ratios are given; based on this, the ratios have been calculated (Table 3).

Table 2: Mean ± one standard deviation of dissolved organic N and dissolved organic P concentrations and nutrient ratios. The other nutrient concentrations can be found in Table 1 of the main text.

	Control (C)	Light and Phosphorous (L&P)	Fine sediment (FS)	Light and Phosphorous +fine sediment (L&P+FS)
TDN [µg L^{-1}]	1450 ± 18.7	1464 ± 55	1454 ± 32.1	1458 ± 14.8
TDP [µg L^{-1}]	7.6 ± 0.9	46.8 ± 3.1	7 ± 0	50.2 ± 4
DIN [µg L^{-1}]	1055.3 ± 8.5	1046.7 ± 6.2	1052.1 ± 12	1053.3 ± 9.1
DON [µg L^{-1}]	394.7 ± 23.5	417.3 ± 58.1	401.9 ± 40	404.7 ± 22.8
DOP [µg L^{-1}]	6.6 ± 1.2	6.2 ± 0.4	6 ± 0.3	7.8 ± 4.8
bioavail. DOC [µg L^{-1}]	374.1 ± 290.1	572 ± 189.9	650 ± 195.8	1000 ± 1417.7
bioavail. DON [µg L^{-1}]	3.9 ± 0.2	26.4 ± 43.6	15.1 ± 15.9	36 ± 32
bioavail. DOP [µg L^{-1}]	3.3 ± 3.4	1 ± 0.7	2.5 ± 3	3 ± 4.5
DIN : TDN ratio	0.7 ± 0	0.7 ± 0	0.7 ± 0	0.7 ± 0
SRP : TDP ratio	0.1 ± 0.1	0.9 ± 0	0.1 ± 0	0.8 ± 0.1

Table 3: Median reactive molar (µM = µmol L^{-1}) nutrient concentrations and their ratios. Median is chosen because the ratios are log-normal distributed.

	Control (C)	Light and Phosphorous (L&P)	Fine sediment (FS)	Light and Phosphorous +fine sediment (L&P+FS)
Reactive DOC [µM]	28.3	53.3	57.5	41.6
Reactive N [µM]	75.9	75.7	75.8	77.3
Reactive P [µM]	0.2	1.3	0.1	1.5
Reactive DOC : N	0.4	0.7	0.8	0.5
Reactive DOC : P	186.9	40.3	936.6	28.7
Reactive N : P	501.2	57.2	1236.1	53.2
Reactive DOC : N :P	187 : 501 : 1	40 : 57 : 1	937 : 1236 : 1	29 : 53 : 1

The reactive DOC : N ratios are < 1 independent of treatment, whereas the reactive DOC : P ratios are highly dependent on the L&P treatment (Table 3). The ternary plot reveals that the samples are all in the range of C:P co-limitation (lower right corner), which is somewhat alleviated but not removed in the L&P+FS and L&P treatment due to the added SRP. Hence, bacterial uptake of nitrate-N is severely limited by DOC and by reactive P in the treatments without added SRP (Fig. 5). I detected a single outlier for the L&P+FS treatment (a single point close to the center, Fig. 5). The DOC bioavailability of this flume channel was significantly higher (36% bioavailability of the DOC) compared to all other flume channels (on average, 6.9% bioavailability for all flume channels, see also Fig. 5). We cannot explain this outlier; however, we assume it to be a measurement or experimental error since it must have contained a very similar DOC compared to the other flumes.

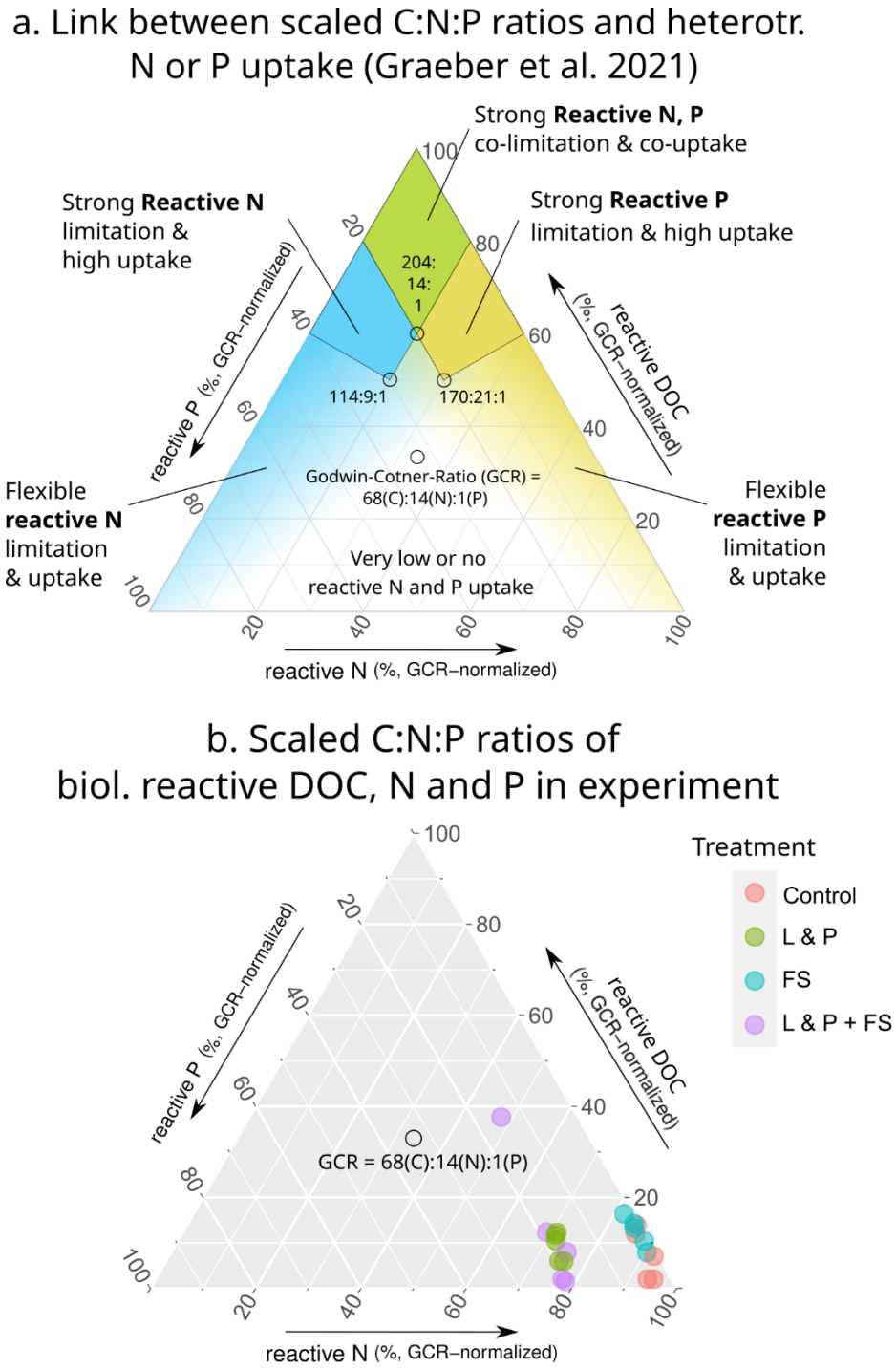

Fig. 5: Ternary plot of relative macronutrient limitation of bacterial reactive N and reactive P uptake. Panel a. shows the conceptual results plot from a microcosm experiment which has proven the strong link between reactive DOC, N and P and the N and P uptake (Graeber et al. 2021). Panel b. shows the relative limitation of the current experiment.

References

Daoud ABA, Tremblay L (2019) HPLC-SEC-FTIR characterization of the dissolved organic matter produced by the microbial carbon pump. Marine Chemistry 215:103668. https://doi.org/10.1016/j.marchem.2019.103668

Fellman JB, D'Amore DV, Hood E, Boone RD (2008) Fluorescence characteristics and biodegradability of dissolved organic matter in forest and wetland soils from coastal temperate watersheds in southeast Alaska. Biogeochemistry 88:169–184

Godwin CM, Cotner JB (2018) What intrinsic and extrinsic factors explain the stoichiometric diversity of aquatic heterotrophic bacteria? The ISME Journal 12:598–609. https://doi.org/10.1038/ismej.2017.195

Graeber D, Gelbrecht J, Kronvang B, et al (2012) Technical Note: Comparison between a direct and the standard, indirect method for dissolved organic nitrogen determination in freshwater environments with high dissolved inorganic nitrogen concentrations. Biogeosciences 9:4873–4884. https://doi.org/10.5194/bg-9-4873-2012

Graeber D, Gücker B, Wild R, et al (2019) Biofilm-specific uptake does not explain differences in whole-stream DOC tracer uptake between a forest and an agricultural stream. Biogeochemistry 144:85–101. https://doi.org/10.1007/s10533-019-00573-6

Graeber D, Tenzin Y, Stutter M, et al (2021) Bioavailable DOC: Reactive nutrient ratios control heterotrophic nutrient assimilation experimental proof of the macronutrient-access hypothesis. Biogeochemistry 155:1–20. https://doi.org/10.1007/s10533-021-00809-4

Helton AM, Ardón M, Bernhardt ES (2015) Thermodynamic constraints on the utility of ecological stoichiometry for explaining global biogeochemical patterns. Ecology Letters 18:1049–1056. https://doi.org/10.1111/ele.12487

Jarvie HP, Smith DR, Norton LR, et al (2018) Phosphorus and nitrogen limitation and impairment of headwater streams relative to rivers in Great Britain: A national perspective on eutrophication. Science of The Total Environment 621:849–862. https://doi.org/10.1016/j.scitotenv.2017.11.128

Kothawala DN, Murphy KR, Stedmon CA, et al (2013) Inner filter correction of dissolved organic matter fluorescence. Limnology and Oceanography-Methods 11:616–630. https://doi.org/10.4319/lom.2013.11.616

Lawaetz AJ, Stedmon CA (2009) Fluorescence intensity calibration using the Raman scatter peak of water. Applied Spectroscopy 63:936–940. https://doi.org/https://www.s-a-s.org/journal/viewer/abstract/597/

Lee WT, Westerhoff P (2005) Dissolved organic nitrogen measurement using dialysis pretreatment. Environmental Science & Technology 39:879–884. https://doi.org/10.1021/es048818y

Murphy KR, Stedmon CA, Graeber D, Bro R (2013) Fluorescence spectroscopy and multi-way techniques: PARAFAC. Analytical Methods 5:6557–6566. https://doi.org/10.1039/C3AY41160E

Pucher M, Wünsch U, Weigelhofer G, et al (2019) staRdom: Versatile Software for Analyzing Spectroscopic Data of Dissolved Organic Matter in R. Water 11:2366. https://doi.org/10.3390/w11112366

Qualls RG, Haines BL (1992) Biodegradability of Dissolved Organic-Matter in Forest Throughfall, Soil Solution, and Stream Water. Soil Science Society Of America Journal 56:578–586

Rodriguez-Cardona B (2015) Nitrate uptake kinetics in streams: Is carbon the driver? Master's Theses and Capstones

Rodríguez-Cardona B, Wymore AS, McDowell WH (2016) DOC:NO3- ratios and NO3- uptake in forested headwater streams. Journal of Geophysical Research: Biogeosciences 121:2015JG003146. https://doi.org/10.1002/2015JG003146

Stutter M, Graeber D, Weigelhofer G (2020a) Available Dissolved Organic Carbon Alters Uptake and Recycling of Phosphorus and Nitrogen from River Sediments. Water 12:3321. https://doi.org/10.3390/w12123321

Stutter MI, Graeber D, Evans CD, et al (2018) Balancing macronutrient stoichiometry to alleviate eutrophication. Science of The Total Environment 634:439–447. https://doi.org/10.1016/j.scitotenv.2018.03.298

Stutter M, Wyness A, Watson H, Dodd N (2020b) Coupled macronutrient cycling in stream biofilms: Effects of stoichiometry, light and temperature. Science of the Total Environment 703: https://doi.org/10.1016/j.scitotenv.2019.134880

Taylor PG, Townsend AR (2010) Stoichiometric control of organic carbonnitrate relationships from soils to the sea. Nature 464:1178–1181. https://doi.org/10.1038/nature08985

Thompson S, Cotner J (2020) P-limitation drives changes in DOM production by aquatic bacteria. Aquatic Microbial Ecology 85:35–46. https://doi.org/10.3354/ame01940